

Hydrothermal Synthesis of ZnO Nano-Disks

**S. Gauthameshwar
Roll.No. 1811069**

Sixth Semester Project Report



Under the supervision of **Dr. Pratap Kumar Sahoo**
School Of Physical Sciences
National Institute Of Science Education and Research
Bhubaneswar,Jatni

2021

Abstract

An attempt to synthesise Zinc Oxide nano-disks using hydrothermal process and to identify the optimal conditions to obtain such nano-disks is made. We have tried suppressing the longitudinal growth of Zinc Oxide nano-rods using Chlorine chemistry, adjusting OH-ion concentrations, and by introducing small organic molecules like citrate ions in our solution to obtain nano-disks from the more commonly obtained nano-rod structures of ZnO. The first two methods could not be optimised to obtain disks whereas the latter gave acceptable results. But due to unfavorable COVID circumstances, the optimisation could not be completed and analysed thoroughly. The UV-visible spectra and the the Photo-luminescence (PL) properties of the samples were however taken.

Acknowledgements

I wish to express my heartfelt gratitude towards **Dr. Pratap Kumar Sahoo** for guiding me in my 6th semester project by spending significant amount of time making me familiarise in the ways of an experimentalist and always providing me the needed motivation to continue with my experiments. I would like to thank my senior Bhavesh Sarangi for helping me with the experiments, providing the necessary procedure and precautions. I would like to thank Utkalika P Sahoo for her guidance, time, and particularly helping me with obtaining FESEM, EDAX data of my samples. I would like to thank Mrinal Kanti Sikdar and Subhashree Sahoo assisting me in PL instruments and Sputtering system needed for seed layers. I would like to thank all my labmates including Bidyadhar Das, Gurupada Ghorai, Sourav Bhakta, Kalyan Ghosh and Dr. Madhusmita Sahoo for creating a positive atmosphere throughout my project. Last but not the least, I thank my parents for their supporting me in pursuing this project amidst these testing times.

Contents

Abstract	ii
Acknowledgements	iii
List of Figures	vi
1 Introduction	1
1.1 General Information on ZnO and its applications	1
1.2 Hydrothermal synthesis of ZnO nanodisks	2
1.3 ZnO Structure	3
2 Experimental Section	5
2.1 Batch 1: Obtaining Zinc Oxide Nanorods	5
2.2 Batch 2: OH suppression to obtain Nanodisks from Nanorods	6
2.3 Batch 3: Varying concentrations of Zinc Acetate-HMTA in 1:1 ratio .	7
2.4 Batch 4: Chlorine Chemistry and doping of Organic Molecules	8
2.5 Batch 5: Continuation of Batch 4	9
3 Analysis Techniques Used	10
3.1 Field Emission Scanning Electron Microscope (FESEM)	10
3.2 Photoluminescence	11
3.3 UV-Visible Spectroscopy	12
4 Experimental Result and Discussion	14
4.1 Batch 1	14

4.2	Batch 2	16
4.3	Batch 3	16
4.4	Batch 4	19
4.5	Batch 5	21
4.6	UV-Visible	23
4.7	Photoluminescence data	25
4.8	Discussion	26
4.8.1	ZnO Nanorods	26
4.8.2	Twin rods from 0.01M ZnAc soln	26
4.8.3	Ineffectiveness of Chlorine chemistry and OH-suppression	27
4.8.4	Effect of too much citrate	29
5	Conclusion	31
6	Bibliography	33

List of Figures

1.1	Samples of Zinc Oxide nanodisks prepared from CVD method	2
1.2	Schematic of Hydrothermal process of synthesising ZnO crystals	3
1.3	Wurtzite ZnO structure	3
1.4	Top view of wurtzite ZnO	4
1.5	A Hexagonal Bravais Lattice	4
3.1	Mechanism of FESEM	11
3.2	Schematic for PL	12
3.3	Schematic of UV-Visible spectrometer	13
4.1	SEM image of crystals formed in the top substrate	15
4.2	SEM image of crystals formed in the middle substrate	15
4.3	SEM image of crystals formed in the Bottom substrate	15
4.4	SEM image of crystals formed in 1:5 $Zn(NO_3)_2$ and HMTA	16
4.5	0.01M ZnAc and HMTA	17
4.6	0.04M ZnAc and HMTA in a seeded substrate	18
4.7	5% NaCit in ZnAc and HMTA	19
4.8	5% NaCl in ZnAc and HMTA	20
4.9	5% LiCl in ZnAc and HMTA	20
4.10	NaCit samples at different concentration of citrate doping	21
4.11	The Final batch with their respective concentrations	22
4.12	Tauc plot of ZnO Nanodisks	23
4.13	Tauc plot of ZnO Nanorods	24
4.14	Tauc plot of ZnO twin rods	24

4.15 PL spectra of different samples	25
4.16 Comparison of Nanorods formed in Batch 1 and Batch 5	26
4.17 General setup for formation of twin rods.	27
4.18 Structure of citrate ion	28
4.19 Zn surrounded by citrate ions	29
4.20 Comparison of ZnO samples formed in 10% and 15% citrate soln . . .	30

Chapter 1

Introduction

1.1 General Information on ZnO and its applications

Zinc oxide is an extremely versatile material that has variety of interesting properties that has made it one of the most studied materials in research. It has found various uses in low threshold UV lasers, piezoelectric devices, transistors and LEDs [1]. It has interesting opto-electric properties owing to it's direct wide band gap (3.4eV) in the range of a semiconductor, and large exciton binding energy (60MeV) [2]. Even more interestingly, it can be synthesised to varieties of shapes and sizes to achieve a specified purpose by controlling its growth conditions. Thus, ZnO can morph itself to several shapes in the nanoscale [3]. This drastically changes their distinct physical, chemical, optical and mechanical properties. Nanorods, Nanowires, Nanotubes, Nano-twin rods are some examples of the forms ZnO crystals can take [4].

We are specifically interested in synthesising ZnO nanodisks. Two most common ways of synthesise it are Chemical Vapor Deposition (CVD), and Hydrothermal method. ZnO nanodisks have direct application in lasers, Josephson Junctions and vertically aligned ZnO nanodisks can even be used in bulk hetrojunction photovoltaic [8]. Thus it might be beneficial to synthesise these disks in a cost efficient hydrothermal method.

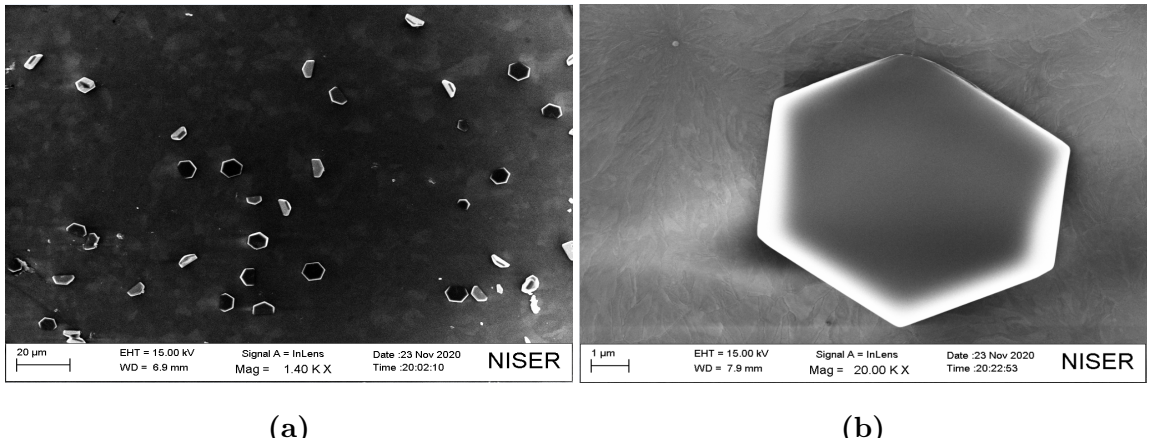
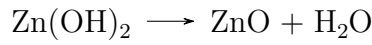
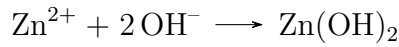
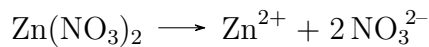


Figure 1.1: Samples of Zinc Oxide nanodisks prepared from CVD method

1.2 Hydrothermal synthesis of ZnO nanodisks

In hydrothermal method, a zinc salt, such as $Zn(NO_3)_2$ or $Zn(CH_3COO)_2$ is kept in a basic solution such as NH_4OH or HTMA ($(CH_2)_6N_4$) that results in the formation of Zinc hydroxide in the solution. Upon heating, these zinc hydroxide crystallise into ZnO. The reaction mechanism for a Zinc nitrate salt is given below:



Introducing organic molecules or changing the pH of the solution directly affects the morphology of the crystals formed. The reaction occurs in a sealed container with an either seeded or unseeded silica substrate (SiO_2) which is collectively placed in a heat bath at a constant temperature between $60 - 95^\circ C$. Schematic of this

process is given in Fig.1.2

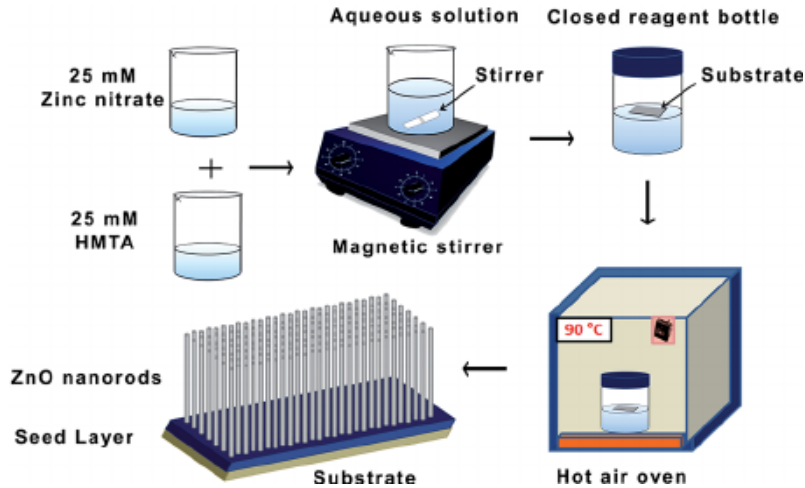


Figure 1.2: Schematic of Hydrothermal process of synthesising ZnO crystals

1.3 ZnO Structure

ZnO primarily has three structures. Wurtzite, Zinc Blende and rocksalt. Wurtzite is the most common of them all due to its thermodynamic stability in configuration compared to the other two. Wurtzite is a hexagonal Bravais lattice with two basis atoms (Zn and O) in a single primitive lattice. Each Zinc atom is tetrahedrally connected to its neighbouring oxygen atoms in sp³ covalent bond, making the coordination number n=4. A typical Hexagon Bravais lattice and the structure of ZnO computed in VESTA is given below in Fig 1.2-1.4:

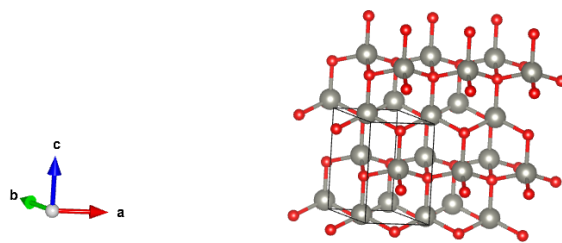


Figure 1.3: Wurtzite ZnO structure

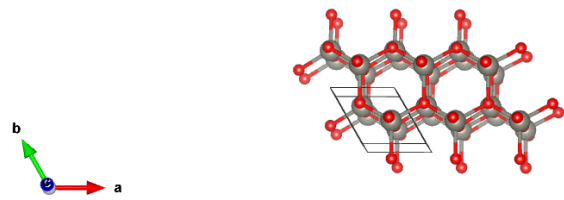


Figure 1.4: Top view of wurtzite ZnO

Wurtzite ZnO has lattice parameters $a = 3.28910 \text{ \AA}$, and $c = 5.30682 \text{ \AA}$ in its conventional unit cell. It exhibits ABABAB stacking along z-axis as in any ideal hexagonal lattices.

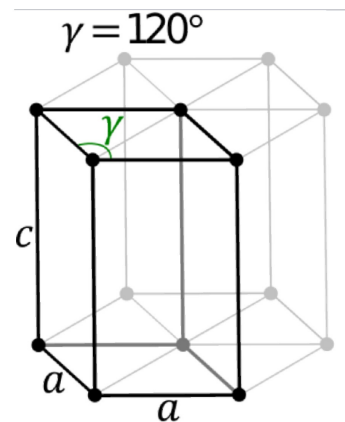


Figure 1.5: A Hexagonal Bravais Lattice

Chapter 2

Experimental Section

We have made batches of samples that used two different types of seeding for promoting crystal growth:

- Dropping method: In this method of seeding, a solution of Zinc Oxide is made by mixing 1.5 gm of Zinc Oxide nanopowder to 100ml DI water and stirred for 15 mins. The obtained solution is immediately taken in a dropper, before visible sedimentation is seen and is put on top of the substrate. The substrate is then heated to 200 C for 5 minutes, till the water evaporates, and then allowed to cool to room temperature.
- RF Sputtering: In this method, Zinc Oxide is loaded into the sputtering chamber and the substrates are coated with a thin ZnO film 10 nm.

The preparation of substrate was same for all the batches. Silicon substrate was cut into small pieces. They were cleaned ultrasonically in deionized water, isopropyl alcohol(IPA) and Acetone solutions, each for 5 minutes. After which they are dried by the air blower.

2.1 Batch 1: Obtaining Zinc Oxide Nanorods

In this batch, we aimed to synthesise zinc oxide nanorods from Zinc Nitrate in a basic environment provided by Hexamethylene tetracetate (HMTA).

1. 0.01M Zn(NO₃)₂.6H₂O soultion is prepared by adding 0.189 gm of salt in 100 ml of water and mixing it in magnetic stirrer for 5 min.
2. 0.01M HMTA solution is prepared by adding 0.140 gm of salt in 100 ml of water and mixing it in magnetic stirrer for 5 min.
3. Both are mixed to obtain a 1:1 ratio solution of Zn(NO₃)₂.6H₂O and HMTA.
4. Three substrates are stuck to a glass slide equally space across the slide, and they are loaded in an airtight container with the solution immersing all the substrates
5. The bottles are placed in a hot water bath at about 85-90° C for 4 hours.
6. After synthesis, the bottles are cooled to room temperature, the substrate was taken out and was rinsed with DI water.
7. After drying it with a blower, it is stored in a plastic container

2.2 Batch 2: OH suppression to obtain Nanodisks from Nanorods

In this batch, we repeat the same procedure as Batch 1 but with a step that is expected to result in suppression of [0001] growth of crystal [2].

The Zinc nitrate and HMTA solutions are prepared as in Batch 1. But now, to obtain a 1:5 ratio of the solutions respectively, 20 ml of 0.01M Zinc nitrate soln is added to 100ml of 0.01M HMTA.

Further, we intend to see the effect of seeding our substrate to the growth of our crystals. So we stick one unseeded and one seeded sample in the glass slide and follow the steps as in Batch 1 to obtain our ZnO crystals.

2.3. Batch 3: Varying concentrations of Zinc Acetate-HMTA in 1:1 ratio

2.3 Batch 3: Varying concentrations of Zinc Acetate-HMTA in 1:1 ratio

This Batch tries to reproduce the results of a paper that suggests the formation of nanodisks under an ambient concentration of Zinc acetate and HMTA taken in 1:1 ratio [2]. We prepare two solutions one with 0.01M concentration of Zinc acetate, and the other with 0.04M concentration. 0.04M concentration is suggested as the ambient concentration for nanodisk formation.

1. 0.01M $\text{Zn}(\text{CH}_3\text{COO})_2$ solution is prepared by adding 0.189 gm of salt in 100 ml of water and mixing it in magnetic stirrer for 5 min.
2. 0.01M HMTA solution is prepared by adding 0.140 gm of salt in 100 ml of water and mixing it in magnetic stirrer for 5 min.
3. 0.04M $\text{Zn}(\text{CH}_3\text{COO})_2$ solution is prepared by adding 0.756 gm of salt in 100 ml of water and mixing it in magnetic stirrer for 5 min.
4. 0.04M HMTA solution is prepared by adding 0.560 gm of salt in 100 ml of water and mixing it in magnetic stirrer for 5 min.
5. Both are mixed to obtain a 1:1 ratio solution of $\text{Zn}(\text{CH}_3\text{COO})_2$ and HMTA.
6. Two substrates, one seeded using dropper method, and the other unseeded are stuck to a glass slide equally space across the slide, and they are loaded in an airtight container with the solution immersing all the substrates. Two such containers with 0.01M and 0.04M solns are made ready for the next step.
7. The bottles are placed in a hot water bath at about 85-90° C for 3 hours.
8. After synthesis, the bottles are cooled to room temperature, the substrate was taken out and was rinsed with DI water.
9. After drying it with a blower, it is stored in a plastic container

2.4 Batch 4: Chlorine Chemistry and doping of Organic Molecules

This Batch explores the chlorine chemistry method that is used to obtain nanodisks in CVD synthesis [5], and a paper that suggests introduction of organic molecules to suppress [0001] growth in the formed ZnO crystals to form disks from rods [3]. We introduce Sodium citrate as the organic molecule into the solution that promotes disk formation.

Three solutions of NaCl, LiCl, and NaCitrate are prepared as follows:

1. 5mM NaCl soultion is prepared by adding 29.22 mg of salt in 100 ml of water and mixing it in magnetic stirrer for 5 min.
2. 5mM LiCl soultion is prepared by adding 21.20 mg of salt in 100 ml of water and mixing it in magnetic stirrer for 5 min.
3. 0.25mM NaCit soultion is prepared by adding 147.05 mg of salt in 100 ml of water and mixing it in magnetic stirrer for 5 min.
4. 5mM Zinc acetate solution is prepared by adding 109.75 mg of salt in 100 ml of water and mixing it in magnetic stirrer for 5 min.
5. 5mM HMTA solution is prepared by adding 70.1 mg of salt in 100 ml of water and mixing it in magnetic stirrer for 5 min.
6. Both the solution of zinc acetate and HMTA are mixed to obtain a 1:1 ratio solution (Sol A) .
7. Sol A is put in three containers with 30 ml soln each. 1.5ml of NaCl and LiCl are added to two of the containers using a pipette. 3 ml of NaCit soln is added to the last container.
8. The bottles are then placed in a hot water bath at about 85-90° C for 3 hours.
9. After synthesis, the bottles are cooled to room temperature, the substrate was taken out and was rinsed with DI water.

10. After drying it with a blower, it is stored in a plastic container

2.5 Batch 5: Continuation of Batch 4

This batch is the final batch that could be synthesised. It is an extension of the Batch 4. Different concentrations of the Cl and citrate doping were tried out to see if any visible suppression in the [0001] growth is seen.

1. 5mM solutions of Zinc acetate and HMTA are prepared as in Batch 4.
2. 5mM solns of LiCl and NaCl are also prepared as in Batch 4
3. 5mM soln of sodium citrate is prepared by adding 147.05mg of salt to 100ml DI water and mixed using magnetic stirrer.
4. 10% doped NaCl, LiCl and NaCit are made by adding 3ml of their 5mM solns to 30ml base solution respectively.
5. 15% doped NaCl, LiCl and NaCit are made by adding 4.5ml of their 5mM solns to 30ml base solution respectively.
6. All the above six solutions are put in water bath at $65\text{--}70^{\circ}\text{C}$, at a temperature lower than Batch 4. The growth duration to crystallise is set to 6 hrs, longer than Batch 4.
7. After 6 hrs, the procedure to clean and store them is same as in Batch 4.

Chapter 3

Analysis Techniques Used

3.1 Field Emission Scanning Electron Microscope (FESEM)

In a field emission (FE) electron microscope, emission of electrons takes place from the conductor (A very thin and sharp tungsten needle) in the presence of a strong Electric field provided by an anode. This pulls the electrons from the conductor and accelerates it towards our sample at high energies. The acceleration voltage between cathode and anode is commonly 0.5 kV to 30 kV. The machine requires an extreme vacuum (around 10⁻⁹ Torr) in the microscope column. The electromagnetic lenses, marked as the condenser lens is used to render the divergent beam into a converging/parallel beam, whereas the focusing lens is used for focusing the beam on the specimen appropriately. The scan coil is then used to focus the beam in a specific point, corresponding to a pixel of the image. The electron beam results in the production of secondary electrons that are emitted by the atoms due to the energetic collisions from the beam. They usually arise from the valence shells of the sample. They are collected by a detector to output the intensity of one pixel in our final image. Repeating the scanning process over the sample surface by repeating the process and scanning all the pixels, we get a high resolution image of the sample. In this project FESEM from ZEISS,Sigma was used to determine the surface morphology of ZnO samples.

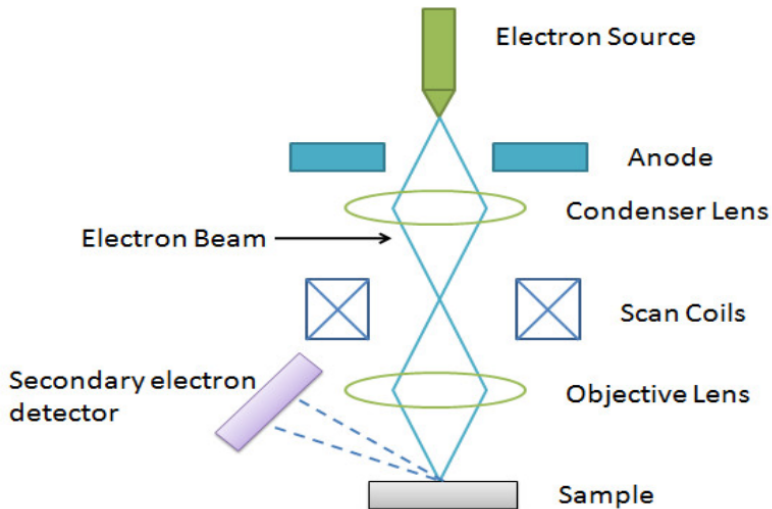


Figure 3.1: Mechanism of FESEM

3.2 Photoluminescence

Photoluminescence (PL) spectroscopy is a non-destructive method of probing the electronic structure of materials. Light is directed onto a sample, where it is absorbed and causes excitation of electrons to higher energy conduction bands along with a production of hole in valence. Once in the conduction band, the electron non-radiatively loses energy to the lowest conduction band energy in the form of crystal phonons. Now, if the band gap is a direct one, we have our electron lose its energy in the form of EM radiations and recombine with its hole in valence band. In the case of photo-excitation, this luminescence is called photoluminescence. The intensity and spectral content of this photoluminescence is a direct measure of various important material properties. The energy of the emitted light (photoluminescence) relates to the difference in energy levels between the two electron states involved in the transition between the excited state and the equilibrium state. In some cases, additional states due to inherent defects or external tampering such as doping might open to which electrons might de-excite to. They can also be analysed from this setup.

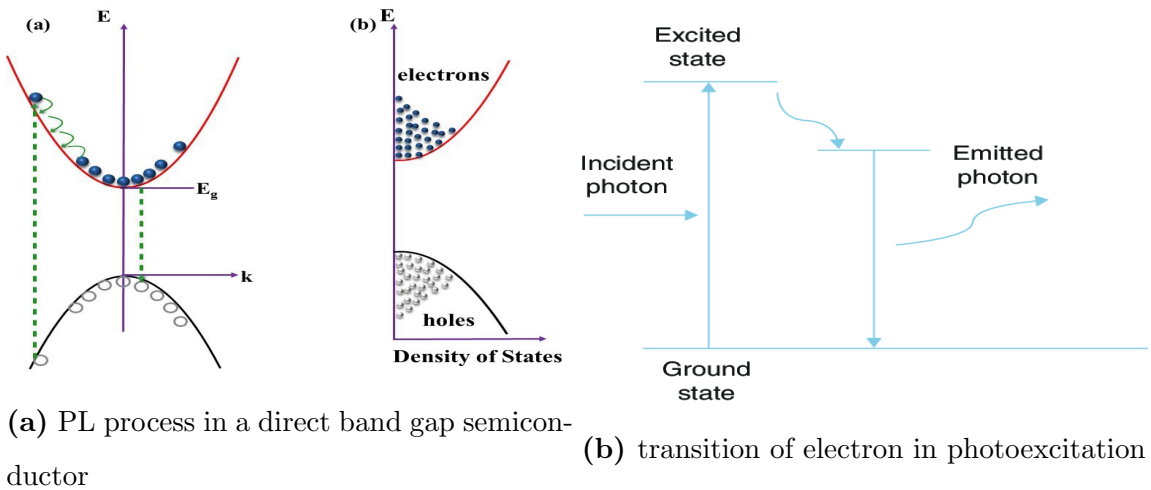


Figure 3.2: Schematic for PL

3.3 UV-Visible Spectroscopy

UV-visible spectroscopy is an important characterisation technique to infer optical properties of a material. It primarily involves tabulating the absorbance of specific wavelengths by the material that lies in the Ultraviolet and Visible range. Our material absorbs light to excite the electrons to unoccupied conduction band from valence band. This net absorbance of photons incident on the sample results in a decrease in the light's intensity as:

$$I_T = I_0 e^{-\alpha d}$$

where I_T, I_0 is the transmitted and incident intensities, d is the sample thickness and α is the absorption coefficient. The UV-Vis absorbance, 'Abs' outputted by the spectrometer is related to α as:

$$Abs = \log(I_0/I_T) = \alpha d$$

The schematic of the UV visible spectroscopy is shown in the Fig below.

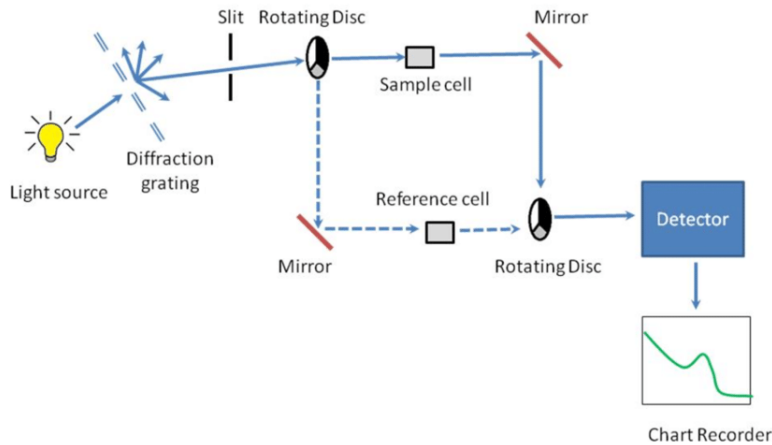


Figure 3.3: Schematic of UV-Visible spectrometer

It turns out that even more useful information can be extracted out of the absorption relation that is obtained from this spectroscopy. The absorption coefficient is related to the wavelength of the absorbed photons as:

$$(\alpha h\nu)^n = \beta(h\nu - E_g)$$

where $h\nu$ is the energy of the incident photon, β is a constant, n depends on the nature of the band gap and E_g is the Energy gap between the Conduction and valence band. For our material ZnO, the band gap is a direct band gap. So the coefficient n becomes 2 in the above equation. So the Tauc plot of the above equation, (i.e), the plot of $(Abs * E)^2$ vs E will have its x-intercept at E_g . Hence, linear interpolation of the linear region of our Tauc plot will give us the direct band gap E_g of our sample.

Chapter 4

Experimental Result and Discussion

4.1 Batch 1

The First batch succeeded in synthesising Nanorods (nothing too surprising). Undoped ZnO nanorods were obtained with dimensions roughly about 400-800 nm in width between opposite hexagon sides and 5-12 μ m in length. The quality of the nanorods were however poor. Some samples were clustered and some had rough sides not grown uniformly across the length.

The samples varied in texture for the three substrates kept. The sample formed on the top tend to be more properly shaped than those grown in the bottom substrate. This may be due to the presence of a gradient of the concentration of $Zn(OH)_2$ in the base solution. Areas with too much concentration of the zinc hydroxide tend to exhibit uneven and ragged shaped nanorods, due to availability of excessive molecules to crystallise, compared to those areas where concentration is ambient. The temperature is also a key factor in bringing smoothness in the rods. Crystals grown in low temperature for longer duration can help produce better shape in the crystals.

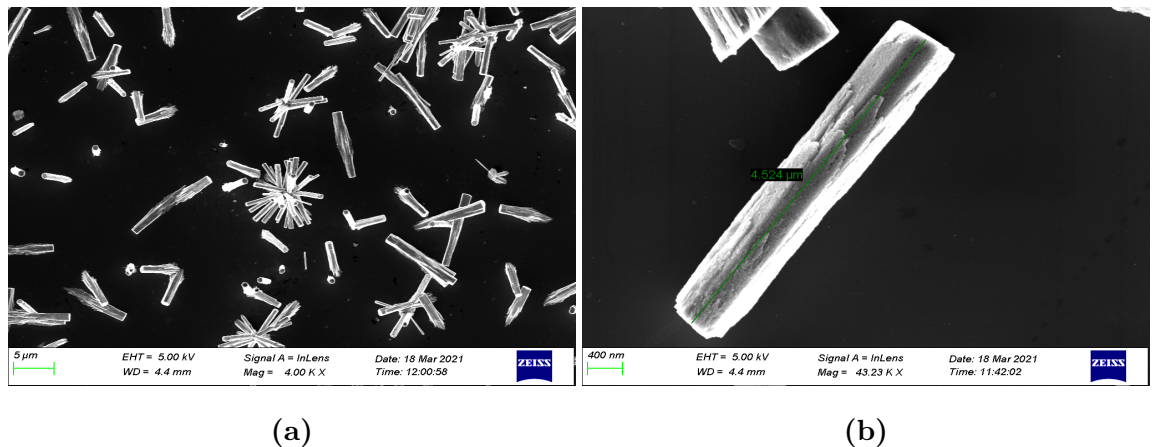


Figure 4.1: SEM image of crystals formed in the top substrate

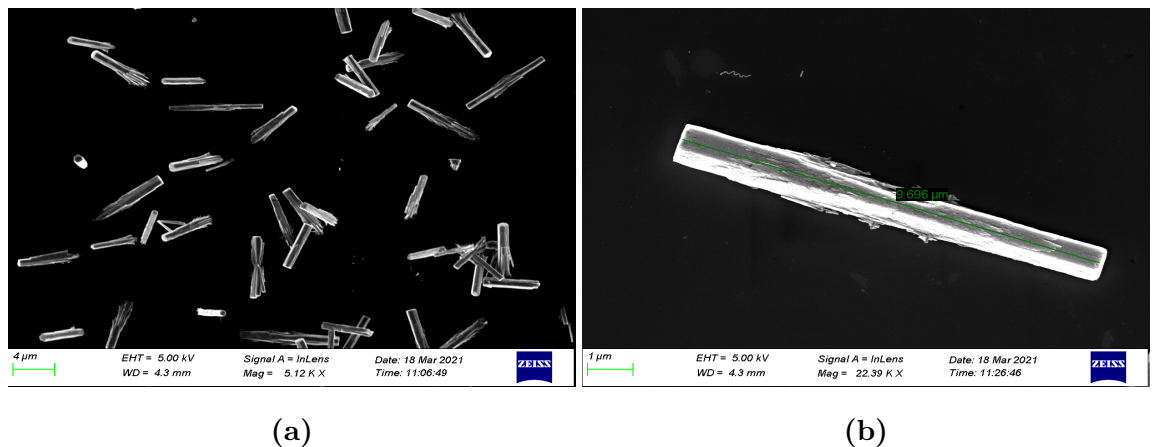


Figure 4.2: SEM image of crystals formed in the middle substrate

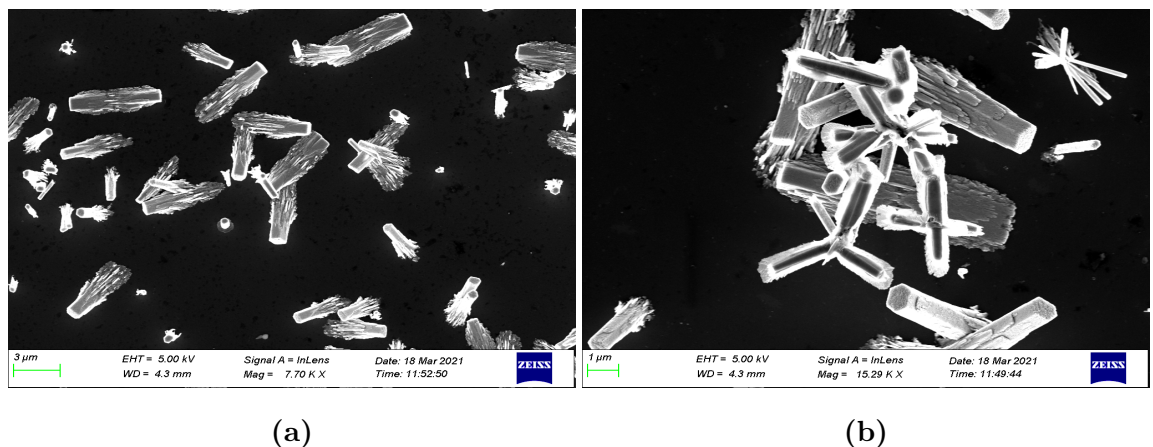


Figure 4.3: SEM image of crystals formed in the Bottom substrate

The vertically aligned crystals are formed on top of the substrate (Those rods where you can see the hexagon face explicitly) and the horizontal ones are formed in the solution that gets stuck to the substrate on drying.

4.2 Batch 2

This batch did not succeed in producing nanodisks. Structures similar to the dimensions of nanorods were observed. A bulge in the middle of most of the rods was observed making it resemble a 'banana'. It could be due to a slight suppression in [0001] direction.

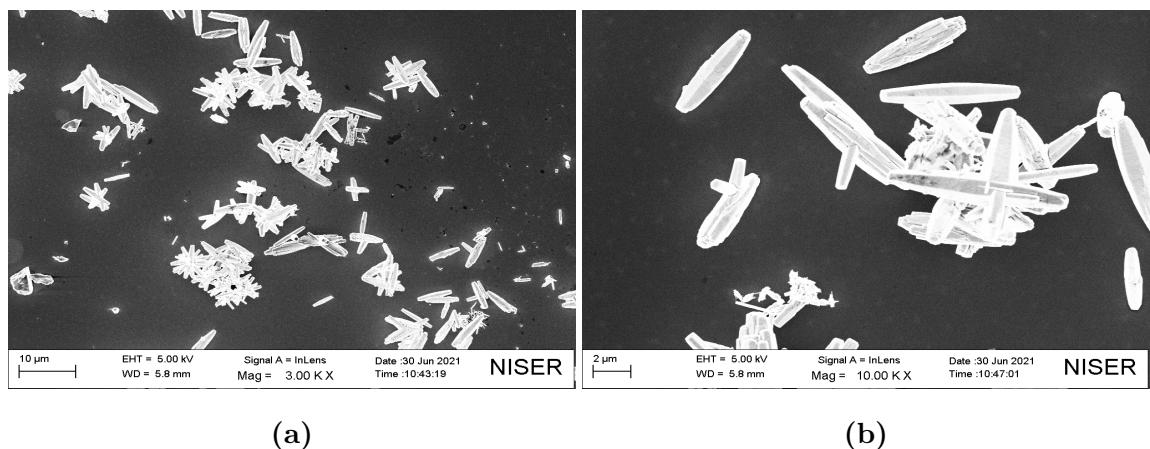


Figure 4.4: SEM image of crystals formed in 1:5 $Zn(NO_3)_2$ and HMTA

Crystals tended to cluster around a nucleation site instead of uniformly forming over the substrate. Perhaps, if we had a proper uniform seed layer, the suppression might have been more prominent.

4.3 Batch 3

This batch did not succeed in forming any disks (or anything even close to it) as predicted and presented in the paper [2]. The two different concentrations of ZnAc and HMTA gave two entirely different shapes of crystals. 0.01M soln had ZnO twin nanorod crystals and the 0.04M soln produced gigantic nanorods. No significant

changes in the crystals formation were seen between seeded and unseeded substrates, unlike the samples produced from Zinc nitrate salt.

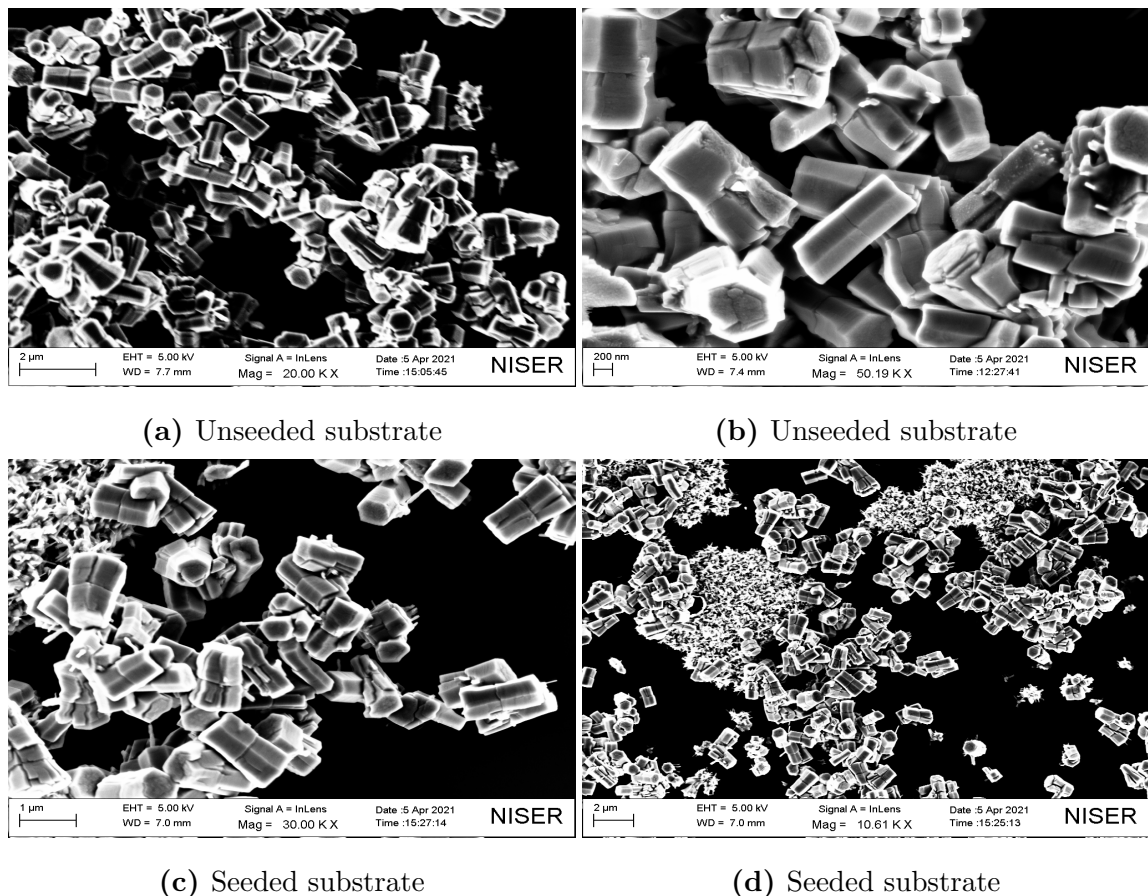


Figure 4.5: 0.01M ZnAc and HMTA

The above samples are quite unevenly formed due to the high (and unstable) temperature of the bath in which they were kept. The dimensions of the crystals varied from 300-800 nm in width and 2-5 μm in length. The dimensions that are quite similar to that of twin nanorods. Besides the twins, additional random and amorphous growth on the seed ZnO sites can also been observed.

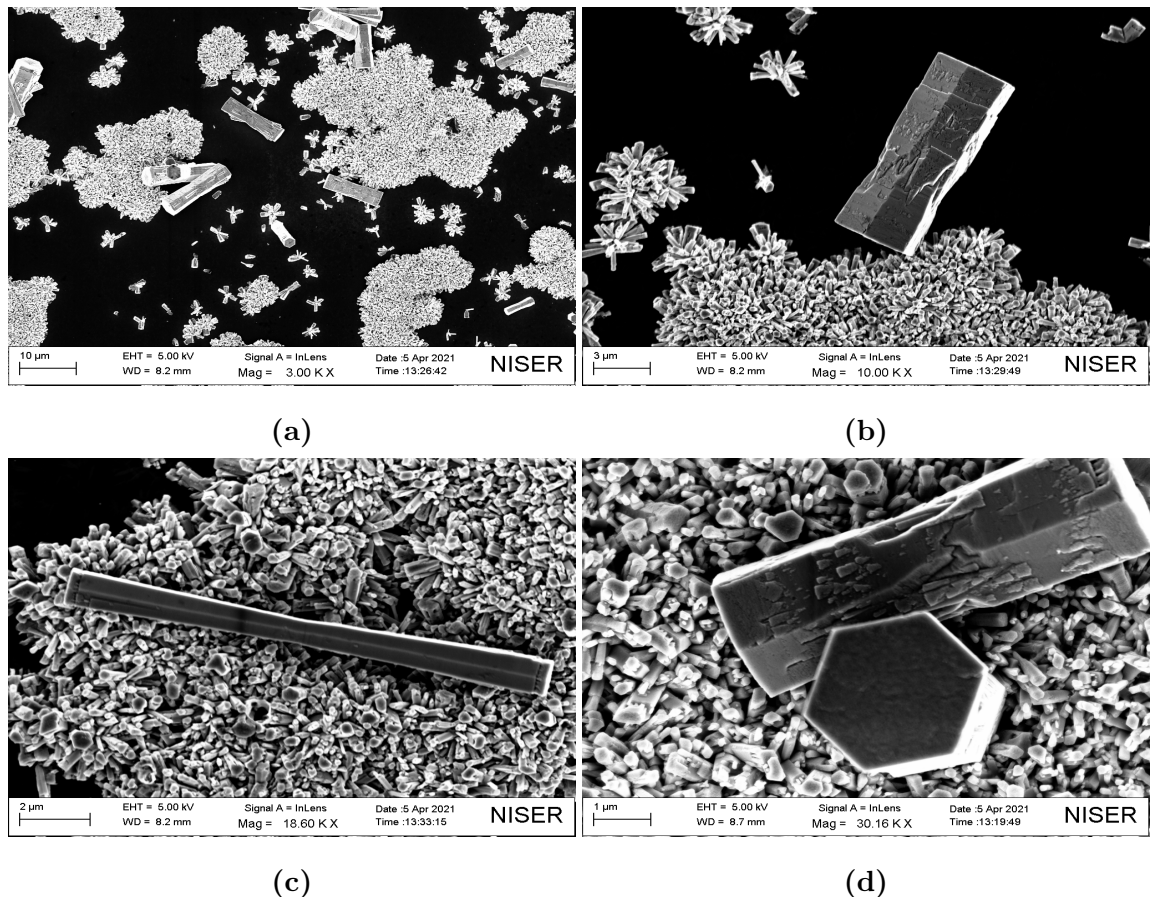


Figure 4.6: 0.04M ZnAc and HMTA in a seeded substrate

The above crystals formed in 0.04M soln exhibited too much growth in all the spatial dimensions. Some crystals grew exceptionally longer in [0001] direction, and some grew wide and bulky, going beyond the ideal dimensions of nanorods in either case. The dimensions fluctuated significantly from crystals. In width, they varied from 1.5-6 μm . The length can be seen anywhere between 10-25 μm . The samples can be safely named "Microrods" instead of "Nanorods" since even the smallest dimension is in μm . The effect of seeding in the substrate again did not bring any significant change in the crystals formed.

4.4 Batch 4

This batch successfully managed to obtain thick ZnO nanodisks in the 5% doped Sodium citrate soln. The 5% doped NaCl and LiCl did not produce any observable suppression in [0001] axis.

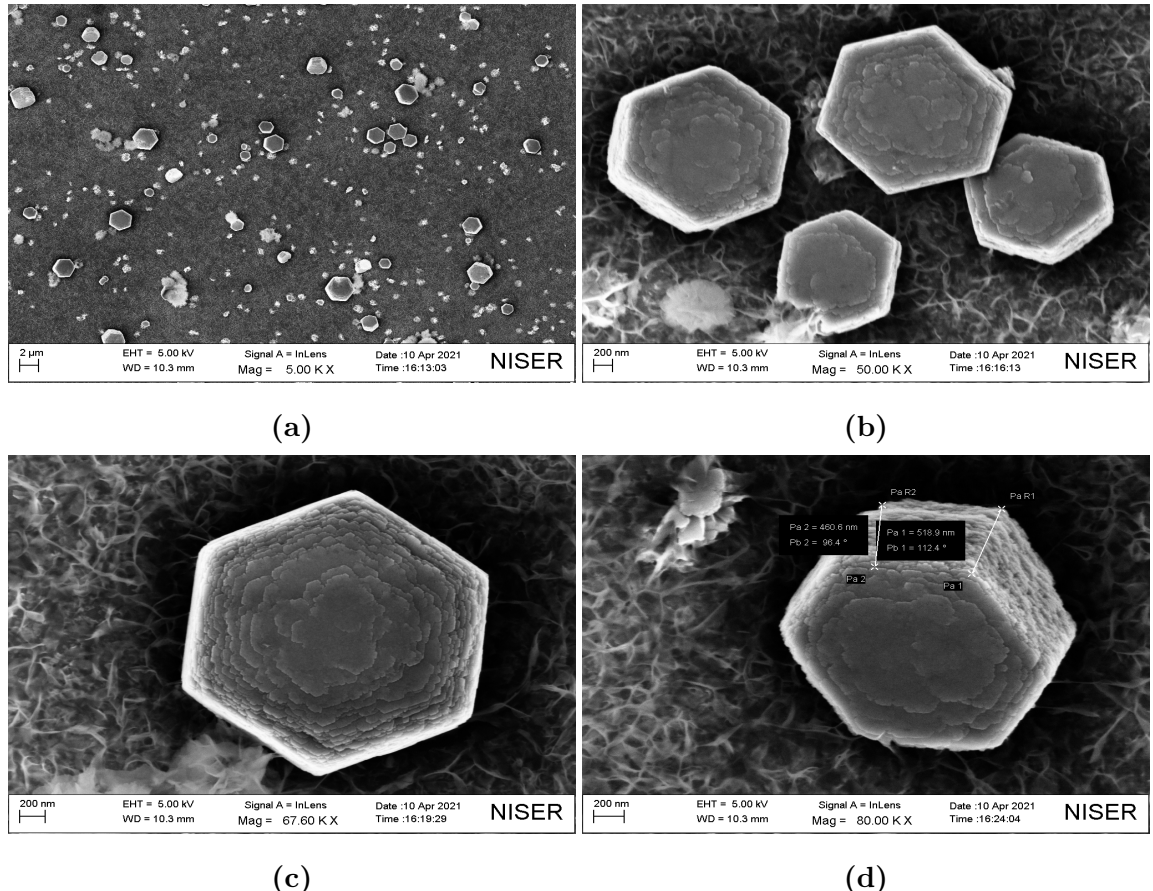


Figure 4.7: 5% NaCit in ZnAc and HMTA

The Nanodisks formed had the width in the range 1-3 μm and the thickness varying between 300-800 nm. A significant suppression in [0001] growth is (finally!) seen in this sample resulting in larger dimensions of width in the crystal. A layer by layer growth is also visible in the disks.

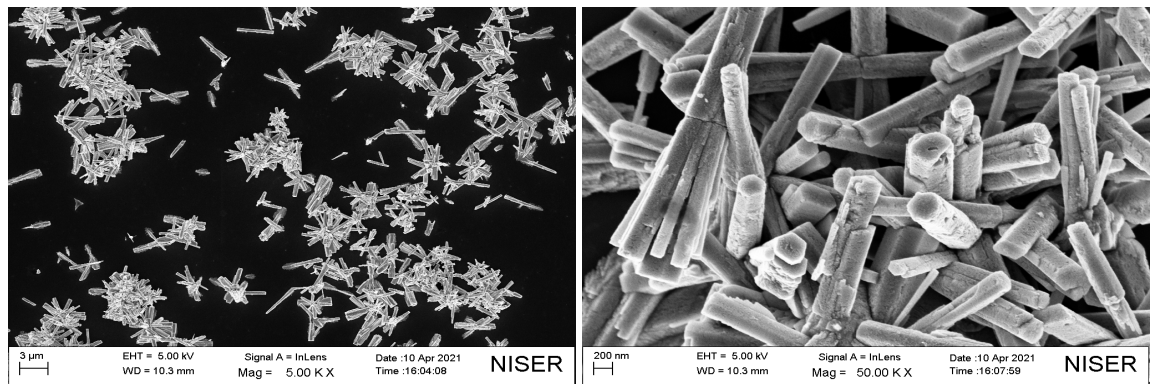


Figure 4.8: 5% NaCl in ZnAc and HMTA

Both NaCl (Above) and LiCl (Below) failed to produce any z-axis suppressed crystals. Nanorods formed were extremely ragged and uneven probably again due the temperature at which they had to grow. The rods grew without any seeding.

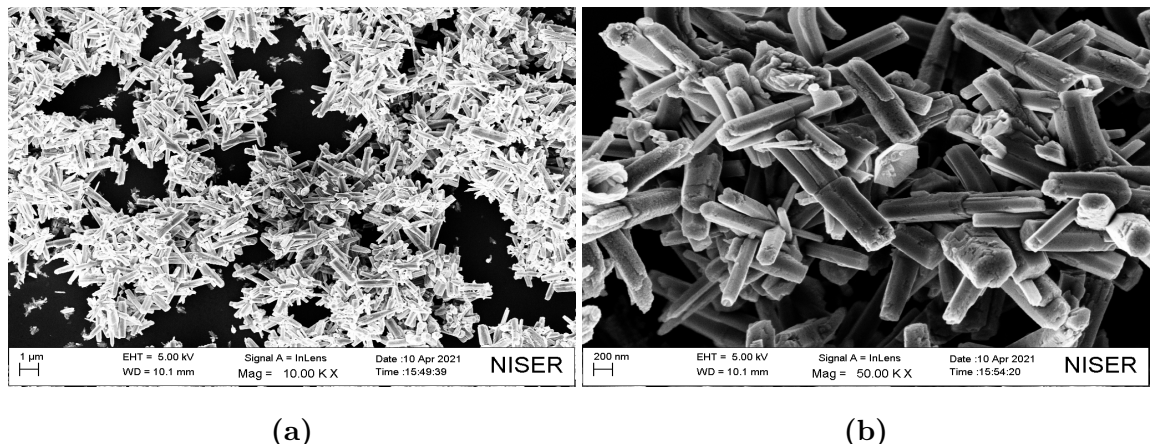


Figure 4.9: 5% LiCl in ZnAc and HMTA

4.5 Batch 5

This Batch was prepared to see if any further increase in Cl-doping might result in any suppression, and to see if any more increase in citrate doping might result in thinner disks. All the above predictions failed. If not any improvement, this batch just turns out to worsen our problem! Increasing the concentration of citrate beyond 5% is seen to provide a poor environment to aid in formation of any crystals. The ZnO formed just grew in lumps and flakes with no proper shape. This effect simply worsens for higher concentrations of doping.

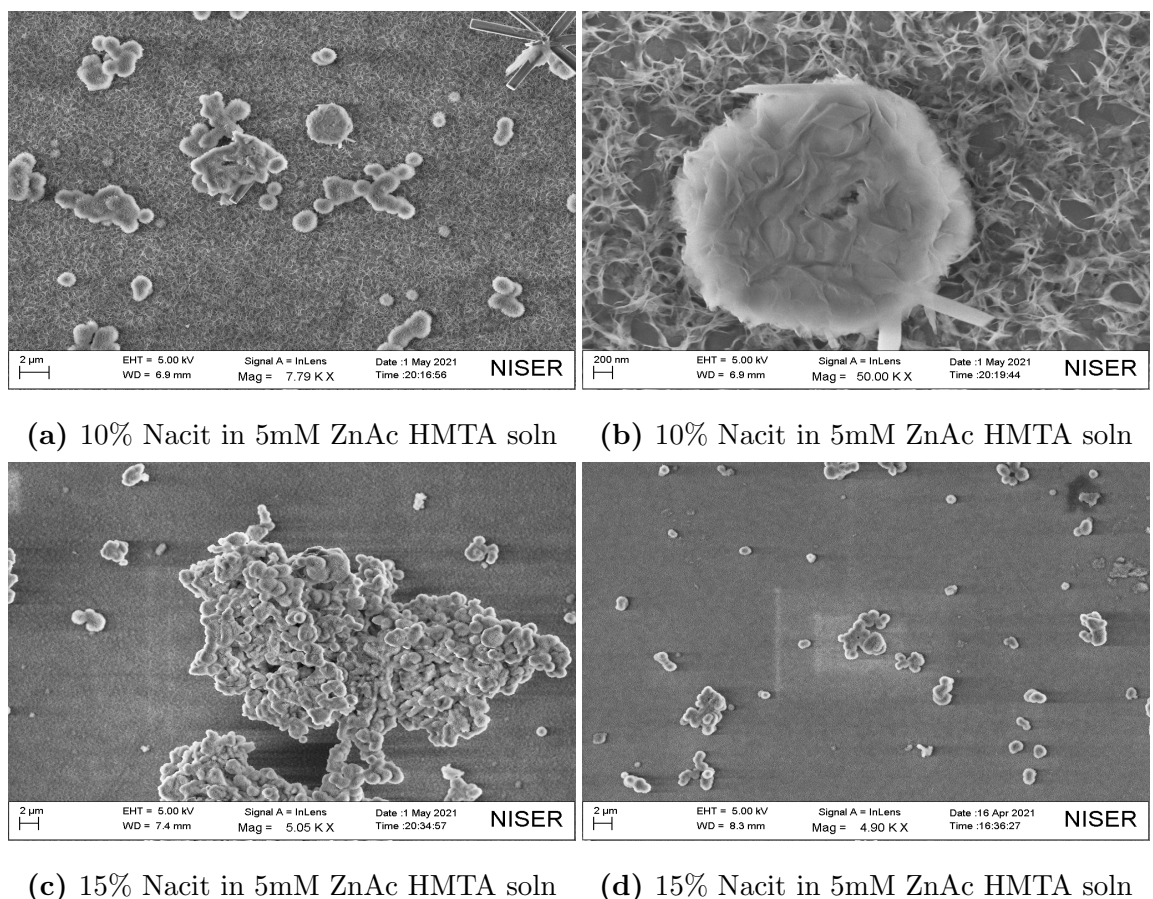


Figure 4.10: NaCit samples at different concentration of citrate doping

Now back to our chlorine chemistry, those samples are simply as redundant as before. Even the slightest suppression in the [0001] axis is not observed on increasing the concentration of Cl^- as large as 15%. Both LiCl and NaCl samples gave almost identical nanorods. Effect of seeding seems ineffective in aiding the growth of the

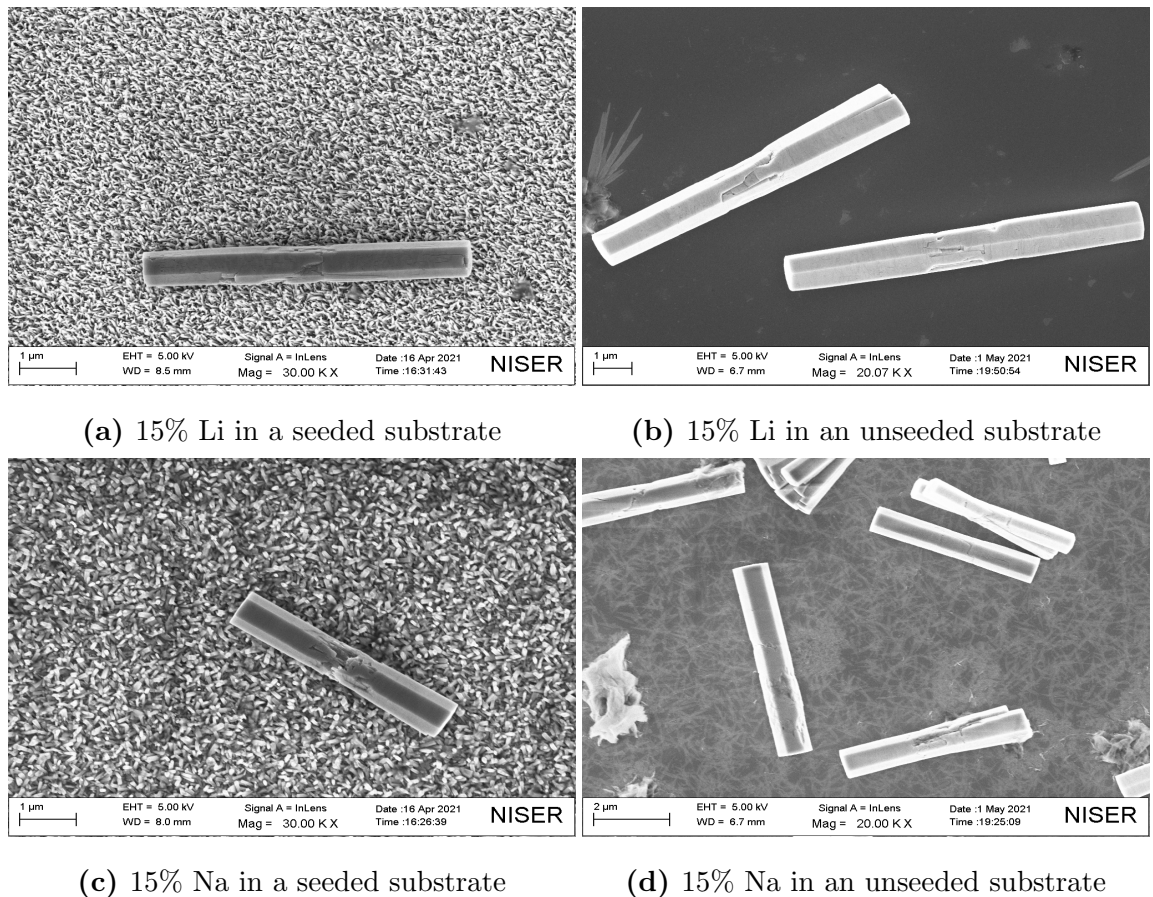


Figure 4.11: The Final batch with their respective concentrations

main nanorods. The crystals seem to grow in the solution and then settle on top of the substrate. Seeding the sample only results in additional growth of minute and ununiform rods with widths around 1-10 nm on top of the seed layer. These truly "nano" rods do not possess any hexagon shaped face unlike their big brothers who lie on top of them. The big nanorods formed, however looks more well shaped than the previous samples, indicating the effectiveness on changing the temperature and duration of crystallisation.

4.6 UV-Visible

The Tauc plots from the Absorption spectra for different incident photon energies is plotted below for all three kinds of ZnO crystal shapes we intentionally (or accidentally) obtained. The linear region extrapolated in the plots yield Band Gap energy of 3.42eV, 3.35eV, 3.35eV for disks, rods and twins respectively. This band gap is a direct one as predicted since it gives a decent linear plot in the absorption region from our theoretical Tauc equation for direct band gap absorption.

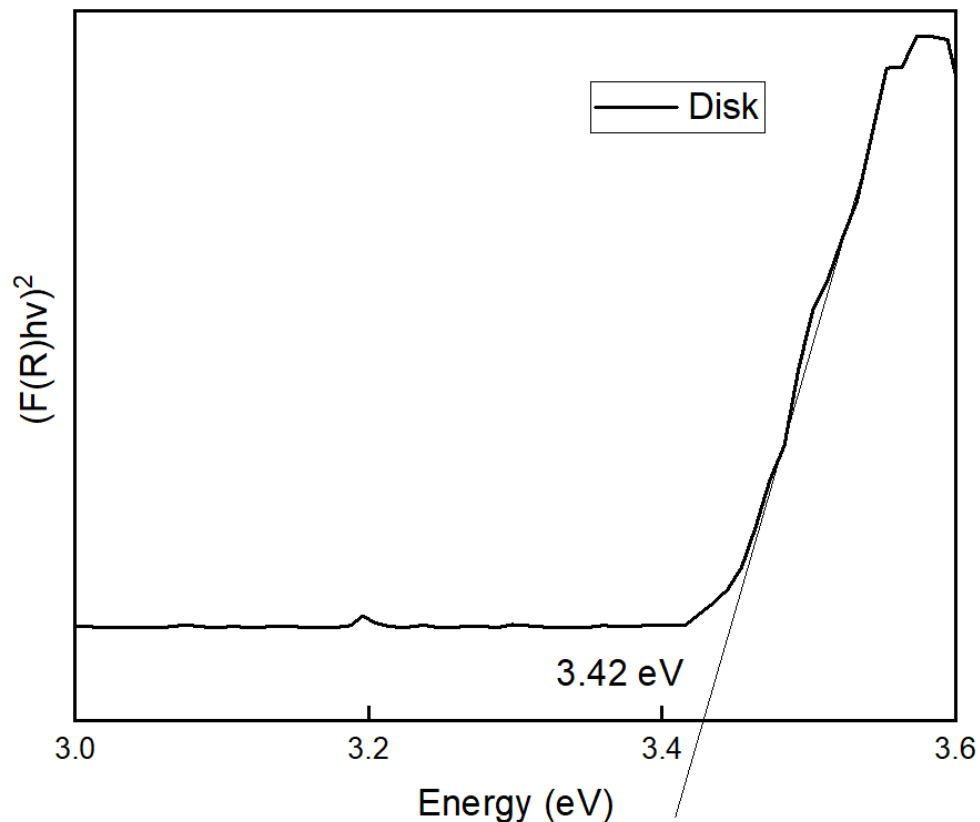


Figure 4.12: Tauc plot of ZnO Nanodisks

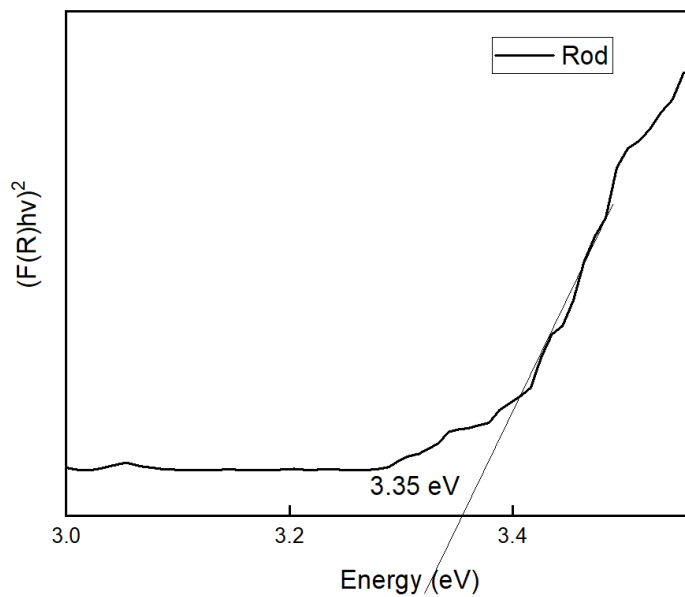


Figure 4.13: Tauc plot of ZnO Nanorods

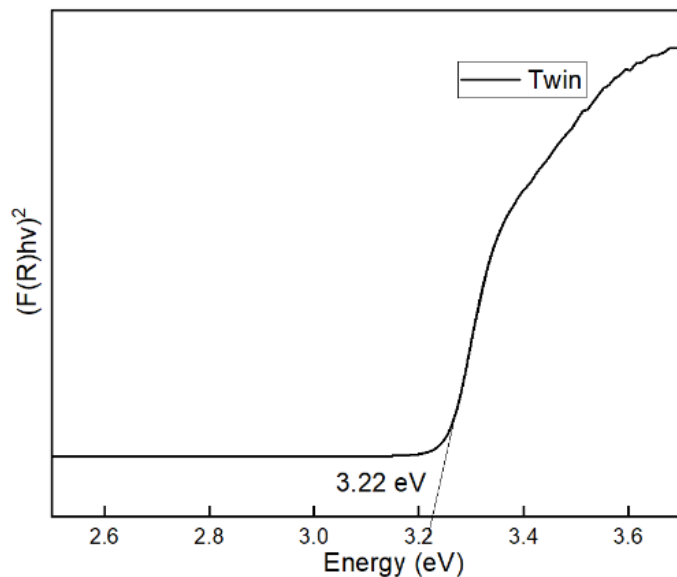


Figure 4.14: Tauc plot of ZnO twin rods

4.7 Photoluminescence data

The PL intensity vs photon energy (converted to eV) is shown below for all three kinds of ZnO crystal shapes.

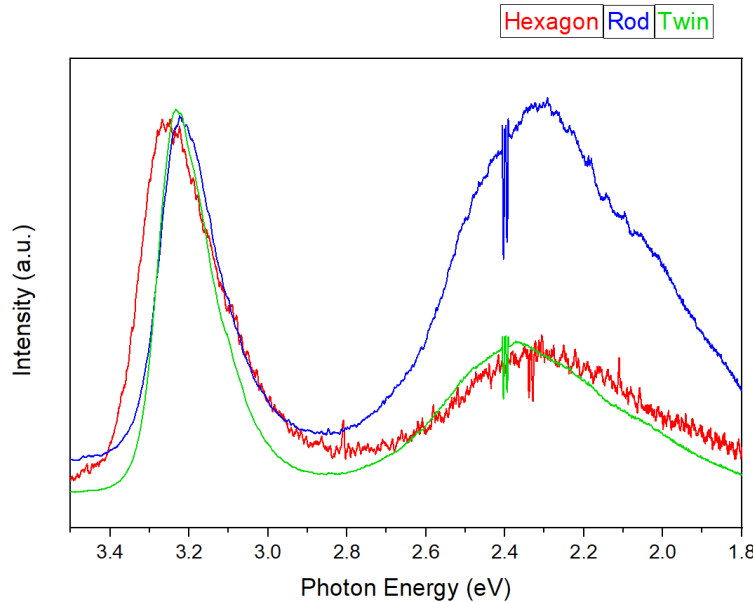
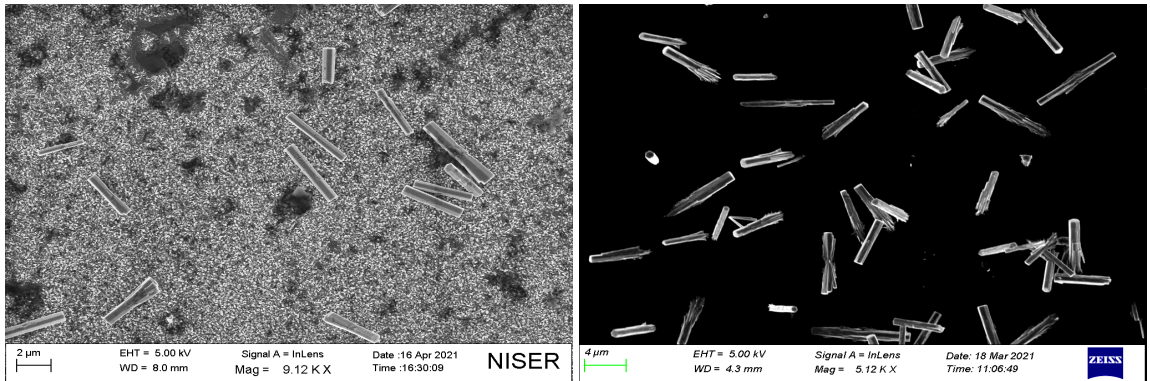


Figure 4.15: PL spectra of different samples

The near band emission peaks are observed around 3.2-3.4eV. We know its Near band emission peak from our UV visible data analysis which predicted the direct band gap energy of our samples. The twin and rod samples almost have the same near band peak at around 3.22eV. The Disk, has a peak shift towards a slightly higher energy of 3.85eV. A broad defect peak besides the near band emission peak is also observed in the green light wavelength range extending to red light range. The defect peak is predicted to occur due to the presence of interstitial vacancy defects in the ZnO crystals [9]. This can be confirmed by the fact that the nanorod grown in 15% Na solution has a more produced defect peak due to more interstitial defects due to Na^+ and O^- ions.



(a) Nanorods in ZnAc soln with 15% Na (b) Nanorods in undoped Zinc nitrate soln

Figure 4.16: Comparison of Nanorods formed in Batch 1 and Batch 5

4.8 Discussion

4.8.1 ZnO Nanorods

The first batch used Zinc Nitrate as the salt to synthesise ZnO crystals. The crystals showed rugged shapes being rough and tapered along the crystal. This suggests Zinc nitrate is sensitive to the temperature at which it is forming crystals. The samples that had zinc acetate preferred to grow in the solution itself instead of nucleating from the substrate, unlike zinc nitrate samples who grew vertically on the substrates as well. It turns out from rods prepared in Batch 5 that keeping the temperature in ambient condition of about 60-70 °C and providing longer crystallisation time leads to smoother and much more evenly shaped nanorods.

4.8.2 Twin rods from 0.01M ZnAc soln

Twin rod formation is strongly influenced by the presence of seed crystals and a convection current [6]. In this batch, the temperature at which the crystals grew was unstable. Due to misreadings in a digital thermometer, the actual temperature of the bath was underestimated and the temperature ramped up to 95° C and very close to boiling temperature of water. Tiny bubbles already started to form from nucleation sites in the substrate and a convection current was set in the solution. At these temperatures, Ostwald ripening becomes a spontaneous process [6]. Thus,

the Zinc hydroxide clusters in the solution readily converts into ZnO crystals and provides small nucleation sites within the solution irrespective of the presence of seeding in the substrate. This leads to the formation of small twin nanorods in both the seeded and unseeded samples in 0.01M ZnAc soln. ZnO crystals can indeed become unpredictable and elusive if proper care is not taken in synthesising them.

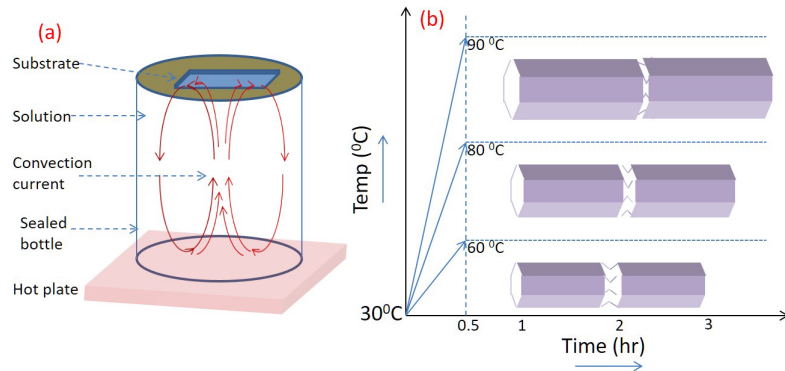


Figure 4.17: General setup for formation of twin rods.

The ideal setup for growth of twins is given in Fig.4.15. We did not have the experimental setup in Fig.4.15. But if certain conditions like the ones discussed above meet, that can also promote formation of twins. [4] The amorphous region in the middle is formed in the sub-crystalline regime where $Zn(OH)_2$ converts to ZnO below the desired reaction temperature $T_r \approx 50^\circ$ [6]. If the temperature in the bath is stable enough, the ramping of the solution temperature inside the vial will be significant enough to prevent the formation of an amorphous growth that results in the formation of twin rods.

4.8.3 Ineffectiveness of Chlorine chemistry and OH-suppression

We have obsessively tried to obtain nanodisks from Chlorine chemistry and OH^- suppression method. Sadly, every attempt to get our much coveted crystal structure is a failure. To explain the reason to this, we try to throw light as to why a suppression by adsorption of anionic species is expected in the first place.

In CVD growth, ZnO is formed on the substrate by subsequent wetting of ZnO vapors on the crystals resulting in a layered disk formation [7]. It is formed under

inert Ar atmosphere and follows direct condensation of ZnO vapors onto the crystals surface without any intermediate product (like $Zn(OH)_2$).

Now we come back to hydrothermal ZnO formation. Since we have our crystals form in a basic solution, we can't ignore the effect of the ZnO crystals being surrounded by OH⁻ ions and the point of zero charge. The point of zero charge (pzc) for ZnO is 9.0 each crystal in a pH = 7.6 solution develops a positive charge on its surfaces. This charge should lead to significant adsorption of anionic species which is ionized in aqueous solutions and carries negatively charged coordination sites. [1] If the surface charge density depends on the crystal face, then the adsorbed species that inhibits or enhances growth, changes in growth rate would be face-specific. But this explanation puts both Cl^- and citrate ions on equal grounds. We expect a suppression in the [0001] face due to its abundant positive surface charge. But citrate ion has its multiple chelating sites and its spatial orientation of carboxylic groups that makes it much more efficient in exhibiting face selective suppression than the chlorine ions. [4]

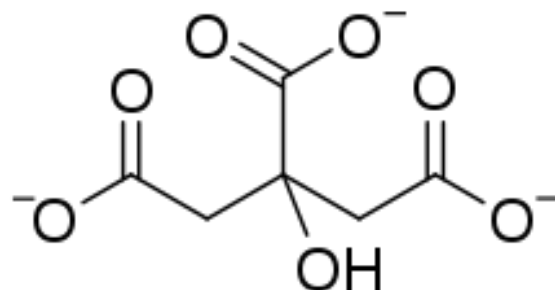


Figure 4.18: Structure of citrate ion

The relative positions of its three carboxylate groups allows little flexibility, making coordinative binding with the crystal surface highly sensitive to the surface's molecular structure, which is face-specific. It can be hypothesized that citrate binds strongly with 0001 crystal faces (which possess threefold rotational symmetry) but weakly with 100 faces (which do not) and that axial growth is therefore drastically suppressed (through a blocking process) compared to equatorial growth. Anions like Cl^- or Acetate don't have that much effect in suppressing [0001] plane on the same surface charge argument. This might be due to the small and univalent nature

of these ions which make it much more easy to displace out of the surface due to thermal agitation or rapid exchange of ions in the solution [4]. Therefore, it can be concluded that introduction of small anions like Cl^- is an ineffective way to suppress [0001] growth in the Zinc oxide formation. OH^- or Cl^- suppression might work if proper seeding of the sample is done using sputtering or sol-gel method where uniform layer of ZnO seed is present throughout the crystal and the crystals are constrained to grow on the substrate unlike our case where crystals tend to form in the solution itself.

4.8.4 Effect of too much citrate

Batch 5 demonstrated that increasing citrate ions in the solution beyond a concentration leads to no proper formation of crystals. This can be explained by the strong chelating property of citrate ion. Due to its multi-carboxylic groups, it can have strong coordination bonds with positive ions. If the concentration is ambient, it will chelate to the surface of the axial ZnO suppressing its growth in that direction. But on finding it in excess, it can now try to form coordination bonds with the Zn^{2+} ions in the solution [4].

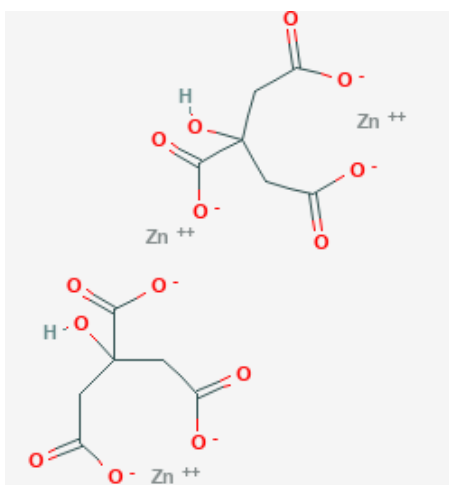


Figure 4.19: Zn surrounded by citrate ions

This chelating effect on Zn^{2+} ions will lead to a net reduction in those ions in the solution and in turn reduce the supersaturation in the solution that is required to form ZnO crystals. Thus, the deficiency of the Zn^{2+} ions in solution will result

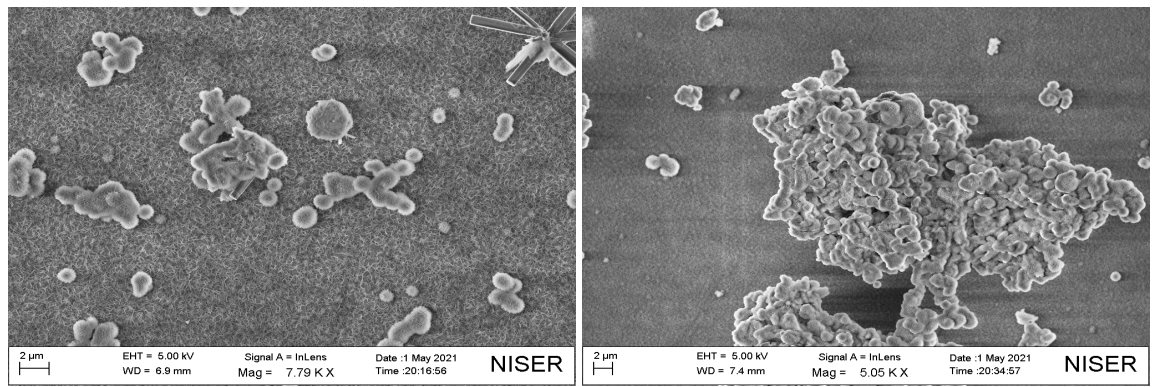


Figure 4.20: Comparison of ZnO samples formed in 10% and 15% citrate soln

in stunted and amorphous growth of ZnO crystals instead of promoting it. This explains why the ZnO crystals lose its morphology for increased concentrations of citrate in our ZnAc-HMTA solution.

Chapter 5

Conclusion

We have been able to explore three methods that is expected to yield our wanted ZnO nanodisk structures.

- OH-suppression seems inefficient in synthesising nanodisks in hydrothermal process and so is Chlorine chemistry to suppress the [0001] axis growth of more commonly obtained ZnO nanorods. OH-suppression neither showed effect on increasing the concentration of 1:1 ZnAc and HMTA nor on making OH ions more available by making 1:5 ratio of ZnAc and HMTA. Pushing up to the limits of 15% doping of Cl^- also proves inefficient in producing even the slightest change in the crystals dimensions.
- It has also been observed that seeding (dropper method) has no effect whatsoever in the shape of the crystals formed. The nanorods are seen to form in the solution and settle on top of the substrate rather than growing on top of the substrate itself, which can suggest using more cheaper substrate like glass over the more expensive silica wafers to hold our nano-crystals.
- The doping of organic molecules is a more hopeful way to introduce changes in the morphology in our crystals. In particular, the doping of citrate ions brought fruitful results in suppressing our [0001] axis growth and result in shape similar to a nanodisk. It is observed, however that increasing the concentration beyond a point (5%) results in unwanted Zn^{2+} titration, creating Zn-deficiency and resulting in loss of crystalline shape of the sample formed.

- It is generally seen that keeping the temperature constant around 70-80°C and allowing it to grow for a longer time is optimal for smooth growth of the crystals.
- The near-band emission of all the three shapes we synthesised came out to be roughly around 3.2-3.9eV in the UV range, as expected from our UV-visible Tauc plot, and the defect peak formed in the green-red region depends on the concentration of impurities that can create stoichiometric defects in our sample formed.

Future Plan

1. Explore the introduction of organic molecules in our solution to bring morphological changes in the crystals formed.
2. Doping ferromagnetic materials like Fe, Co, Ni to study layer-by layer growth of ZnO in hydrothermal process as an extension of results obtained in CVD method.
3. Study of Whispering modes of hydrothermally obtained samples and finding its applications in lasing [10].
4. Use of our ZnO nanodisks in cerating Josephson junctions.

Chapter 6

Bibliography

- [1] Nathan Johann Nicholas, George V. Franks and William A. Ducker. *The mechanism for hydrothermal growth of zinc oxide.* CrystEngComm, 2012, 14, 1232
- [2] Yuanyuan Lv, Zhiyong Zhang, Junfeng Yan, Wu Zhao, Chunxue Zhai, Jin Liu. *Growth mechanism and photoluminescence property of hydrothermal oriented ZnO nanostructures evolving from nanorods to nanoplates.* Journal of Alloys and Compounds 718 (2017) 161e169
- [3] Prabhakar Rai, Sudarsan Raj, In-Hwan Lee, Woon-Ki Kwak, Yeon-Tae Yun. *Conversion of ZnO microrods into microdisks like structures and its effect on photoluminescence properties.* Ceramics International 39 (2013) 8287–8291
- [4] Simon P. Garcia, and Steve Semancik. *Controlling the Morphology of Zinc Oxide Nanorods Crystallized from Aqueous Solutions: The Effect of Crystal Growth Modifiers on Aspect Ratio.* Chem. Mater. 2007, 19, 4016-4022
- [5] Ramin Yousefi, A.K.Zak, M.R.Mahmoudian. *Growth and characterization of Cl-doped ZnO hexagonal nanodisks.* Journal of Solid State Chemistry 184 (2011) 2678–2682
- [6] Ph.D thesis, Avanendra Singh, SPS,NISER (2018)
- [7] L.W. Yanga, X.L. Wua, Y. Xiong, Y.M. Yanga, G.S. Huang, Paul K. Chu, G.G. Siu. *Formation of zinc oxide micro-disks via layer-by-layer growth and*

- growth mechanism of ZnO nanostructures.* Journal of Crystal Growth 283 (2005) 332–338
- [8] Congkang Xu, Kaikun Yang, Liwei Huang, and Howard Wang . *Vertically aligned ZnO nanodisks and their uses in bulk heterojunction solar cells.* Journal of Renewable and Sustainable Energy 2, 053101 (2010)
- [9] X. L. Wu, G. G. Siu and C. L. Fu, H. C. Ong *Photoluminescence and cathodoluminescence studies of stoichiometric and oxygen-deficient ZnO films.* Appl. Phys. Lett. 78, 2285 (2001)
- [10] Daniel J. Gargas, Michael C. Moore, Adrian Ni, Shu-Wei Chang, Zhaoyu Zhang, Shun-Lien Chuang, and Peidong Yang. *Whispering Gallery Mode Lasing from Zinc Oxide Hexagonal Nanodisks.* ACS Nano 2010 4 (6), 3270-3276